Actinometric and Φ–order photodegradation properties of anti–cancer Sunitinib.

Mounir Maafi*, Lok Yan Lee

Leicester School of Pharmacy, De Montfort University, The Gateway, Leicester LE1 9BH, UK

Corresponding Author:
E-mail: mmaafi@dmu.ac.uk;
Tel.: +44 116 257 7704;
fax: +44 116 257 7287.

Abstract

The photodegradation reaction of Sunitinib (SUT), occurring via Z–E photoisomerization, has been evaluated in this study using the recently developed Φ–order kinetics. In ethanol, the forward (Z → E) photoreaction of SUT was invariant with irradiation (its quantum yield, $\Phi_{Z\rightarrow E}^{\lambda_{irr}} \approx$ 0.019) in contrast to the E → Z isomerisation whose $\Phi_{E\rightarrow Z}^{\lambda_{irr}}$ undergoes a 30-fold, sigmoid–shaped, increase with increasing irradiation wavelength. This situation limited usefully the extent of Z–SUT photodegradation at the photostationary state to a maximum of *c.a.* 30 % of the initial concentration. Nevertheless, these results support a strong recommendation for a complete protection of SUT from light at all stages. Furthermore, a SUT-actinometer was developed and was proven to be useful for the 320–480 nm spectral range. The latter wavelength interval defined as well SUT photodegradation causative range. The formalism of Φ–order kinetics, proves to be a useful investigative tool for drugs' photodegradation studies.

Keywords:

Sunitinib, photodegradation, spectrokinetics, quantum yield, photoisomerism, actinometry.

1. Introduction

Z–Sunitinib malate [N-[2-(diethylaminino)ethyl]-5-[(Z)-(5-fluoro-2-oxo-1,2-dihydro-3*H*-indol-3-ylidene)-methyl]-2,4-dimethyl-1*H*-pyrrole-3-carboxamide L-malate], (Z–SUT), is an orally active multiple tyrosine kinase and angiogenesis inhibitor [1,2]. It is part of a new emerging cancer targeted therapies which are characterised by a unique mechanism of action and a high specificity for key biological pathways involved in the cancer process [3]. It is prescribed for metastatic renal cell carcinoma and for the treatment of gastrointestinal stromal tumors [4-5]. Some results suggested that Z–SUT might be active against breast cancer and its efficacy and toxicity do not appear to be affected by patient age, including children and elderly [4]. Its presence in patients skin and sweat was evidenced [6], and its effects in skin photoirritation and phototoxicity have also been reported [7].

A few literature reports indicated its sensitivity to light [8,9]. The mostly descriptive data available thus far, reveals that Z–SUT photodegradation consists of a photoisomerization around the double bond linking the 2–oxyindole and the pyrrole rings leading to E–SUT as a single identified photoproduct in organic media, Scheme 1 [8]. The anti–cancer drug was however found to be thermally stable in methanol in the dark [3,8,9]. Despite Z–SUT recognized photodegradation, a number of studies did not report on practical handling precautions that should have been taken to protect the solutions from light during preparation and analysis [3,6,10-12].

To the best of our knowledge, there are no published kinetic studies on the photodegradation of Z–SUT [13-15]. Zhao et al. Studied the effects of various solvents on the degradation of Z–SUT, and Etienne-Grimaldi et al., reported that Z–SUT phototransformation was completed within 5 minutes of exposure to ambient light in methanolic solutions, but no treatment of the kinetic data was proposed in both these studies [8]. Also, the quantum yields of the photoreaction steps have not yet been reported for this drug.

Recently, a new method of studying photoreversible reactions of drugs has been proposed [16,17]. This type of systems, labelled here AB(2Φ), involves two photoactive species (A and B) each transforming into the other through a single photoprocess characterized by a specific quantum yield (Φ), Scheme 1. Under non-isosbestic irradiation, the overall photoreaction obeys Φ–order kinetics. A description of the mathematical framework of such a reaction is provided in later sections.

The photoreversible reaction is a process responsible for many drugs' degradation [13] and a basis for a number of pharmaceutical and technological systems [18-20]. However, little is known on the reactivity attributes of such processes, especially on their photochemical yields.

The Φ–order kinetic approach [16,17,21], presents a double advantage in proposing a simple mathematical set of equations that simplifies the treatments of the data and provides tools to facilitate both the determination of reaction quantum yields, the quantification of many reactivity aspects, in addition to allowing the prospection and development of new drug–

actinometers. In this respect, Φ–order kinetics stands as a better alternative to the classical treatments using thermal reaction orders.

In this study, the photokinetics of SUT is investigated with the aims of characterizing its reaction photochemical quantum yields relative to the irradiation wavelength and its potential for actinometry.

2. Materials and methods

2.1. *Materials*

Sunitinib maleate, (Z–SUT), and spectrophotometric grade ethanol were purchased from Sigma–Aldrich (Dorset, UK).

2.2. Monochromatic continuous irradiation

An Ushio 1000 W xenon arc-lamp light source housed in a housing shell model A6000 and powered by a power supply model LPS–1200, was used for the irradiation experiments. The setting was cooled by tap water circulation through a pipe system. The lamp housing was connected to a monochromator model 101 that allows the selection of specific irradiation wavelenghths since it consists of a special f/2.5 monochromator with a 1200 groove/300 nm blaze grating. The excitation beam was guided through an optical fibre to impinge from the top of the sample cuvette i.e. the excitation and the analysis light beams were perpendicular to each other. The set up was manufactured by Photon Technology International Corporation (London, Ontario, Canada).

2.3. The monitoring system

A diode array spectrophotometer (Agilent 8453) was used to measure the various absorption spectra and kinetic profiles for the irradiation and calibration experiments. This spectrophotometer was equipped with a 1–cm cuvette sample holder and a Peltier system model Agilent 8453 for temperature control. As such, the sample was kept at 22°C, stirred continuously during the experiment, and almost completely shielded from ambient light. The spectrophotometer was monitored by an Agilent 8453 Chemstation kinetics–software (Agilent Technologies, Lakeside, Cheshire, UK).

An Oriel Radiant Power/Energy meter model 70260 was used to measure the radiant power of the incident excitation beams (Darmstadt, Germany).

2.4. Kinetic data treatment

In order to carry out non–linear fittings and to determine best–fit curves, a Levenberg–Marquardt iterative program within the Origin 6.0 software was used (Bucks, UK).

2.5. Chromatographic HPLC measurements

Sunitinib and its photoproduct were separated on a Gemini C_{18} reverse phase column 5 µm, 2.1 x 50 mm (Phenomenex, Cheshire, UK) fitted to a PerkinElmer Series 200 Pump and UV/Vis

Detector, and a 600 Series Link interface. The set up was remotely controlled by TotalChrom software (PerkinElmer, USA).

Separation of Z– and E–isomers was achieved at a flow rate of 1 ml/min with a mobile phase of 67 % water (adjusted to pH 3 with glacial acetic acid) and 33% acetonitrile. An injection loop of 20 µl was used and the detector wavelength was set at 350 nm. The overall run time of the assay was 6 min, the retention times of Z– and E–SUT were 2.17 and 1.84 min, respectively. The linearity range (of the calibration graph, $peak\ area = 5 \times 10^9 \times C + 15376$) ranged between 5 x 10^{-6} and 2.15 x 10^{-4} M.

2.6. SUT solutions

A stock solution of Z–SUT (*c.a.* 3 x 10^{-4} M) in ethanol was prepared by weighing the solid. The flask was protected from light by aluminium foil wrapping and was kept in the fridge. The stock solution served to prepare diluted fresh analytical solutions (*ca.* 9 x 10^{-6} M) for analysis of irradiation experiments at various wavelengths and *ca.* 6 x 10^{-5} M for HPLC analyses.

For actinometric studies, fresh Z–SUT solutions of the same concentrations (*ca.* 9 x 10^{-6} M) were exposed to monochromatic beams of ten different irradiation wavelengths (480, 460, 440, 420, 400, 380, 360, 345, 340, and 320 nm) using a series of different intensities for each wavelength. The kinetic traces were observed at the irradiation wavelength and subsequently fitted with the Φ–order equations.

Experiments were conducted at least in triplicates.

158

159 ## 3. Results and discussion

160

161 ### *3.1. The Mathematical background*

162

163 #### *3.1.1.* Φ–order kinetics for non–isosbestic irradiation

164

165 Usually, the investigations of drugs' photodegradation were performed using 0^{th}–, 1^{st}–, and
166 2^{nd}–order kinetics [14]. The inadequacy of such photokinetic data treatments in quantifying
167 photodegradation reactions was discussed previously [16,21,22]. Instead, the newly proposed
168 approach that was based on Φ–order kinetics, has been proven to faithfully describe the time
169 evolution of the species concentrations or any related quantity such as the medium absorbance
170 [16,17]. The equations of the Φ–order kinetic model apply when the reactive medium is
171 subjected to non–isosbestic and monochromatic irradiation at constant temperature. The Φ–
172 order approach brings three main advantages in that it allows a unique characterisation of the
173 kinetic data, provides an analytical equation for the overall reaction rate–constant and
174 facilitates the quantification of a number of effects. As a result, there is no possibility for
175 multiple interpretations as it has been the case when using the classical thermal treatments
176 where the same set of data could be attributed, for instance, either 0^{th}–order or 1^{st}–order
177 kinetics [14]. Also, the determination of photodegradation quantum yields and/or the
178 establishment of whether a drug is suitable to act as an actinometer were readily and easily
179 achieved using the equations of Φ–order kinetics.

180

The model equations describing Φ–order kinetics for the photoreversible transformation of initial (A) and photoproduct (B) species which are, respectively, characterised by forward (Φ_{AB}) and reverse (Φ_{BA}) quantum yields and where the species are continuously irradiated with a monochromatic beam (whose non–isosbestic wavelength is λ_{irr}) and absorb differently the incident light (P), (i.e., the absorptivities (ε) of the species are different and have non–zero values ($\varepsilon_A^{\lambda_{irr}} \neq \varepsilon_B^{\lambda_{irr}} \neq 0$)), is [16]:

$$A_{tot}^{\lambda_{irr}/\lambda_{obs}}(t) = A_{tot}^{\lambda_{irr}/\lambda_{obs}}(pss) + \frac{A_A^{\lambda_{irr}/\lambda_{obs}}(0) - A_{tot}^{\lambda_{irr}/\lambda_{obs}}(pss)}{A_A^{\lambda_{irr}/\lambda_{irr}}(0) - A_{tot}^{\lambda_{irr}/\lambda_{irr}}(pss)} \times \frac{l_{\lambda_{obs}}}{l_{\lambda_{irr}}} \times Log\left[1 + \left(10^{\left[\left(A_A^{\lambda_{irr}/\lambda_{irr}}(0) - A_{tot}^{\lambda_{irr}/\lambda_{irr}}(pss)\right) \times \frac{l_{\lambda_{irr}}}{l_{\lambda_{obs}}}\right]} - 1\right) \times e^{-k_{A\rightleftharpoons B}^{\lambda_{irr}} \times t}\right] \quad (1)$$

Eq.1 involves only the cumulative observed absorbances ($A_{tot}^{\lambda_{irr}/\lambda_{obs}}$) of the medium which have been measured under the observation ($l_{\lambda_{obs}}$) and not the excitation ($l_{\lambda_{irr}}$) conditions (with $l_{\lambda_{obs}}$ being the optical path length of the monitoring light inside the sample, whereas $l_{\lambda_{irr}}$ is that of the excitation light across the reactive medium). These optical path lengths ($l_{\lambda_{irr}}$ and $l_{\lambda_{obs}}$) are not necessarily equal for a given experiment, and the absorbance of the medium in the excitation conditions (i.e. corresponding to a measurement along $l_{\lambda_{irr}}$) may not be directly accessible. *Log* is the base 10 logarithm.

The coefficients $A_{tot}^{\lambda_{irr}/\lambda_{obs}}(t)$, $A_{tot}^{\lambda_{irr}/\lambda_{obs}}(0)$, $A_{tot}^{\lambda_{irr}/\lambda_{obs}}(pss)$, $A_{tot}^{\lambda_{irr}/\lambda_{irr}}(0)$ and $A_{tot}^{\lambda_{irr}/\lambda_{irr}}(pss)$ in Eq.1 are the measured (along $l_{\lambda_{obs}}$) total absorbances of the medium respectively recorded at reaction time t, at the initial time (t = 0) and at the photostationary state, *pss* (where t = ∞). The reaction medium is monitored while irradiated at a given irradiation wavelength and simultaneously monitored at either a different observation wavelength ($\lambda_{irr}/\lambda_{obs}$) or at the same wavelength ($\lambda_{irr}/\lambda_{irr}$). It is assumed that the reaction is quantitative and proceeds without by-products.

The analytical expression of the exponential factor, $k_{A\rightleftharpoons B}^{\lambda_{irr}}$, in Eq.1 which represents the overall reaction rate–constant, is given by [16]

$$k_{A\rightleftharpoons B}^{\lambda_{irr}} = \left(\Phi_{A\rightarrow B}^{\lambda_{irr}} \times \varepsilon_A^{\lambda_{irr}} + \Phi_{B\rightarrow A}^{\lambda_{irr}} \times \varepsilon_B^{\lambda_{irr}}\right) \times l_{\lambda_{irr}} \times F_{\lambda_{irr}}(pss) \times P_{\lambda_{irr}} = \beta_{\lambda_{irr}} \times P_{\lambda_{irr}} \qquad (2)$$

where $\Phi_{A\rightarrow B}^{\lambda_{irr}}$ and $\Phi_{B\rightarrow A}^{\lambda_{irr}}$ are the forward and reverse quantum yields of the reaction photochemical steps realised at the irradiation wavelength (λ_{irr}); $P_{\lambda_{irr}}$ is the radiant power; $l_{\lambda_{irr}}$ is the optical path length of the irradiation beam inside the sample, and $F_{\lambda_{irr}}(pss)$ the time-independent photokinetic factor expressed as:

$$F_{\lambda_{irr}}(pss) = \frac{1 - 10^{-\left(A_{tot}^{\lambda_{irr}/\lambda_{irr}}(pss) \times \frac{l_{\lambda_{irr}}}{l_{\lambda_{obs}}}\right)}}{A_{tot}^{\lambda_{irr}/\lambda_{irr}}(pss) \times \frac{l_{\lambda_{irr}}}{l_{\lambda_{obs}}}} \quad (3)$$

215

216

217 The $\beta_{\lambda_{irr}}$ in Eq.2 is a proportionality factor between the overall rate–constant and the radiant
218 power.

219

220 *3.1.2. Equation for isosbestic irradiations*

221

222 The equation expressing the temporal variation of the total observed absorbance for
223 monochromatic light–excitation corresponding to an isosbetic point, $\lambda_{irr} = \lambda_{isos}$ (only a few
224 isosbestic points are usually present on the electronic spectra of AB(2Φ) reactions), has been
225 obtained by a closed–from integration [23], as

226

$$A_{tot}^{\lambda_{isos}/\lambda_{obs}}(t) = A_{tot}^{\lambda_{isos}/\lambda_{obs}}(pss) + \left(A_{A}^{\lambda_{isos}/\lambda_{obs}}(0) - A_{tot}^{\lambda_{isos}/\lambda_{obs}}(pss)\right) \times e^{-k_{A\rightarrow B}^{\lambda_{isos}} \times t} \quad (4)$$

227

228 where the different parameters have the same meanings as above (section 3.1.1) except that
229 they are referenced to $\lambda_{isos} = \lambda_{irr}$. Therefore, $k_{A\rightarrow B}^{\lambda_{isos}}$ was worked out from Eq.2 but with the
230 time–invariant photkinetic factor $F_{\lambda_{isos}}$ (replacing $F_{\lambda_{irr}}(pss)$ in Eqs.2 and 3). $F_{\lambda_{isos}}$ was
231 calculated using Eq.3 with the absorbance measured at λ_{isos}, $A_{tot}^{\lambda_{isos}/\lambda_{isos}}$, was used instead of
232 $A_{tot}^{\lambda_{irr}/\lambda_{irr}}(pss)$.

3.1.3. *Elucidation method of SUT* photoreversible reaction

The kinetic elucidation of AB(2Φ) reactions cannot be achieved by only using the equations set out above for both isosbetic and non–isosbestic irradiations because the obtained fitting parameters ($k_{A\rightleftharpoons B}^{\lambda_{irr}}$ or $k_{A\rightleftharpoons B}^{\lambda_{isos}}$) will not be sufficient to work out the values of the three unknowns of the system, namely, the reaction photochemical quantum yield values and the absorption coefficient of the photoproduct at the irradiation wavelength (assuming that none of the latter attributes is available prior to the experiment). Attempts to solve the kinetics using these parameters leads to a degenerate kinetic solution with identifiability and/or distinguishability issues that cannot be resolved [24].

The elucidation method for photoreversible reactions that was proposed in a previous study, can be implemented in three steps [17].

The first step consists of monitoring the photodegradation reaction performed under monochromatic irradiation at an isosbestic point by HPLC. The use of an isosbestic irradiation stems from the fact that at λ_{isos}, the absorption coefficient of the photoproduct is known ($\varepsilon_A^{\lambda_{isos}} = \varepsilon_B^{\lambda_{isos}}$), hence reducing the number of unknowns characterising the reaction to only two ($\Phi_{A\rightarrow B}^{\lambda_{isos}}$ and $\Phi_{B\rightarrow A}^{\lambda_{isos}}$). Therefore, these quantum yields can be determined using the value of $k_{A\rightleftharpoons B}^{\lambda_{isos}}$ (by fitting the concentration profiles supplied by the HPLC experiment with Eq.4), as

$$\Phi_{A\to B}^{\lambda_{isos}} = \frac{k_{A\to B}^{\lambda_{isos}}}{\varepsilon_A^{\lambda_{isos}} \times l_{\lambda_{isos}} \times P_{\lambda_{isos}} \times F_{\lambda_{isos}}} \times \frac{\left(C_A(0) - C_A(pss)\right)}{C_A(0)} \quad (5)$$

254

$$\Phi_{B\to A}^{\lambda_{isos}} = \frac{k_{A\to B}^{\lambda_{isos}}}{\varepsilon_A^{\lambda_{isos}} \times l_{\lambda_{isos}} \times P_{\lambda_{isos}} \times F_{\lambda_{isos}}} - \Phi_{A\to B}^{\lambda_{isos}} \quad (6)$$

255

256

257 The equilibrium constant ($K_{eq}^{\lambda_{isos}}$, Eq.7), is equivalent, for the isosbestic irradiation condition, to
258 the ratio of the values of the quantum yields at λ_{isos}.

259

$$K_{eq}^{\lambda_{isos}} = \frac{k_{B\to A}^{\lambda_{isos}}}{k_{A\to B}^{\lambda_{isos}}} = \frac{C_B(pss)}{C_A(pss)} = \frac{\Phi_{A\to B}^{\lambda_{isos}}}{\Phi_{B\to A}^{\lambda_{isos}}} \quad (7)$$

260

261

262 It is important to notice that $K_{eq}^{\lambda_{isos}}$ is totally independent of the concentration of the initial
263 species. This is important because the concentration used for the HPLC experiment would be
264 most often not suitable (excessive) for quantitative spectrophotometric measurements of the
265 reaction progress. Hence, a lower concentration of the initial species can be used for the
266 second step of the elucidation method which leads to the reconstruction of the full spectrum of
267 the photoisomer (B). This was achieved, for an isosbetic irradiation, using the value of $K_{eq}^{\lambda_{isos}}$,
268 the total spectra of the reactive medium at *pss* ($A_{tot}^{\lambda_{isos}/\lambda_{olis}}(pss)$), and that of the initial species,
269 as

270

$$\varepsilon_B^{\lambda_{obs}} = \frac{(K_{A\rightleftharpoons B}^{\lambda_{isos}} + 1) \times A_{tot}^{\lambda_{isos}/\lambda_{obs}}(pss) - \varepsilon_A^{\lambda_{obs}} \times l_{obs} \times C_A(0)}{l_{obs} \times K_{A\rightleftharpoons B}^{\lambda_{isos}} \times C_A(0)} \quad (8)$$

As a matter of fact, knowing $\varepsilon_B^{\lambda_{obs}}$ (i.e. for any λ_{obs}) reduces the number of unknowns to only two (the reaction quantum yields) irrespective of the irradiation wavelength selected. Therefore, the last step of the method leads to the determination of the absolute values of $\Phi_{A\rightarrow B}^{\lambda_{irr}}$ and $\Phi_{B\rightarrow A}^{\lambda_{irr}}$ at any non–isosbestic/isosbetic irradiation wavelength. $\Phi_{A\rightarrow B}^{\lambda_{irr}}$ can readily be worked out using Eq.9.

$$\Phi_{A\rightarrow B}^{\lambda_{irr}} = \frac{v_{0\,(old.)}^{\lambda_{irr}/\lambda_{obs}}}{\left(\varepsilon_B^{\lambda_{obs}} - \varepsilon_A^{\lambda_{obs}}\right) \times l_{\lambda_{abs}} \times \varepsilon_A^{\lambda_{irr}} \times l_{\lambda_{irr}} \times P_{\lambda_{irr}} \times F_0^{\lambda_{irr}} \times C_0} \quad (9)$$

The numerical value of the reaction initial velocity ($v_{0\,(old.)}^{\lambda_{irr}/\lambda_{obs}}$) involved in Eq.9 could be obtained graphically from Eq.10.

$$v_{0\,(mod.)}^{\lambda_{irr}/\lambda_{obs}} = \frac{A_{tot}^{\lambda_{irr}/\lambda_{obs}}(0) - A_{tot}^{\lambda_{irr}/\lambda_{obs}}(pss)}{A_{tot}^{\lambda_{irr}/\lambda_{irr}}(0) - A_{tot}^{\lambda_{irr}/\lambda_{irr}}(pss)} \times \frac{k_{A\rightleftharpoons B\,(mod.)}^{\lambda_{irr}}}{\frac{l_{\lambda_{irr}}}{l_{\lambda_{obs}}} \times Ln(10)} \times \left(10^{\left(A_{tot}^{\lambda_{irr}/\lambda_{irr}(pss)} - A_{tot}^{\lambda_{irr}/\lambda_{irr}(0)}\right) \times \frac{l_{\lambda_{irr}}}{l_{\lambda_{obs}}}} - 1\right) \quad (10)$$

The value of the final unknown, $\Phi_{B\rightarrow A}^{\lambda_{irr}}$, was then derived from Eq.3.

3.2. Sunitinib photodegradation and Φ–order reaction

The electronic spectra of both SUT isomers present three main absorption regions, 200–240, 240–330, and 330–500 nm. The first and last transitions are characterised by the highest intensities. The long-wavelength band is responsible of absorption in the visible range which gives the colour of SUT solutions.

The continuous irradiation of the initial Z–isomer (Scheme 1) provokes slight changes in absorbance intensities in the 240–330 and 390–490 nm regions (Fig.1). These features indicate the occurrence of chemical transformation, i.e. the degradation of the active isomer. The modest magnitude of absorbance changes might either be due to the similarity between the absorption coefficients of the two isomers or to a low percentage of the E–isomer in solution up to the photostationary state (pss). Nonetheless, the reaction does not seem to produce by–products and evolves smoothly as indicated by the isosbestic points (Fig.1).

SUT ethanolic solutions are thermally stable but react relatively quickly to light, reaching completion in about half an hour when exposed to relatively weak light intensities. This property infers and confirms a strong recommendation to protect this anti–cancer drug from light.

The kinetics of SUT was studied under various monochromatic irradiations that were selected on the main absorption transitions (λ_{irr} = 480, 460, 440, 420, 400, 380, 360,345, 340, 260 and 240 nm). The kinetic profiles representing the temporal variation of the total absorbance of the medium, obtained under the above irradiation conditions (λ_{irr}) and recorded at a unique observation wavelength, λ_{obs} = 445 nm, were consistently fitted by Eq.1 (Fig.2). Therefore, Φ–order kinetics is confirmed for the photodegradation of this anti–cancer drug.

The fitting parameters derived from the application of Eq.1 to the experimental data (Fig.2), correspond to the Z–*E* overall rate–constant values ($k_{A\rightarrow B}^{\lambda_{irr}}$) of SUT photodegradation reaction. The $k_{A\rightarrow B}^{\lambda_{irr}}$ values were found to increase and then decrease with wavelength (Table 1). Such behaviour of $k_{A\rightarrow B}^{\lambda_{irr}}$ doesn't correlate in an evident way with neither the experimental values of $P_{\lambda_{irr}}$ nor those of the initial SUT concentration (Table 1). This observation clearly underlines a real difficulty in using the $k_{A\rightarrow B}^{\lambda_{irr}}$ values for any reliable interpretation about the reactivity of SUT at different wavelengths. It also raises caution, in general, about comparing rate–constant values between different experiments performed in different conditions and/or using different drugs.

This is even a more acute issue if the kinetic data are treated with the equations that have been set out for the classical thermal reaction orders and/or when polychromatic light is employed [16]. Therefore, the photodegradation kinetics must be elucidated with the aim to determine the values of all reactivity attributes.

3.3. SUT kinetic elucidation

The photodegradation of SUT performed using a monochromatic and isosbestic (345 nm) irradiation was monitored by HPLC. The only photoproduct identified in solution alongside the initial species has been attributed to the E–SUT isomer. The concentration profiles of E– and Z–SUT isomers, obtained in these conditions (Fig.3), indicate that the latter mainly contributes to the composition of the photostationary state as less than 25 % of Z–SUT has transformed into its geometric isomer at the reaction completion (pss). This feature corroborates the small magnitude of change on the absorbance recorded on the spectrokinetic traces (Figs.1 and 2). The concentration profiles are well fitted by first–order equations for photoreversible reactions derived from Eq.4 (Fig.3). The value of the overall photodegradation rate–constant ($k_{A\rightleftharpoons B}^{\lambda_{isos}}$) was obtained as the fitting parameter. Accordingly, the values of the forward ($\Phi_{A\rightarrow B}^{345}$) and reverse ($\Phi_{B\rightarrow A}^{345}$) quantum yields at the isosbestic irradiation can be worked out from Eq.5 and Eq.6, respectively (Table 2). The Z to E photoisomerisation is found to be more than 3–fold less efficient than its reverse counterpart with an equilibrium constant of 0.315. The higher concentration of the Z–SUT at pss corroborates the general trend observed for cis–trans isomerization [17,25] and can also be justified in the case of SUT by a more extensive steric congestion in the E–isomer due to the spatial vicinity of the benzenic and pyrrolic rings which most likely leads to a non–planar molecule. Anyway, in ethanol, the small value of $K_{\rightleftharpoons}^{\lambda_{isos}}$ (0.315) due to smaller Z → E and higher E → Z photoisomerization quantum yields, advantageously limits the extent of Z–SUT photodegradation to a maximum of *c.a.* 30 % of the initial concentration.

The full spectrum of the photoproduct, E–SUT can now be retrieved by applying Eq.8 using the observed spectrum of the medium which was recorded at *pss* ($A_{tot}^{\lambda_{sss}/\lambda_{obs}}(pss)$) together with the value of the equilibrium constant $K_{\lambda}^{\lambda_{isos}}$ (Table 2). The electronic spectra of the two isomers overlap throughout the range of absorption with the Z–SUT being characterised by higher values of the absorption coefficients everywhere except in the 230–270 nm region where a new absorption band appeared (λ_{max} = 250 nm, Log(ε) = 4.3) replacing the original weak unresolved spectrum in the 240–330 nm region.

The values of quantum yields for both Z–SUT and E–SUT unimolecular phototransoformations can be derived from Eqs. 9 and 2 for any non-isosbestic wavelength (Table 3, Fig.5). The quantum yield of the forward (Z $\rightarrow$ E) photoreaction ($\Phi_{A\rightarrow B}^{\lambda_{irr}}$) is relatively low and insensitive to irradiation wavelength as the values collected for the selected wavelengths, spanning 220 nm (480-240 nm), were spread around their mean, $\Phi_{A\rightarrow B}^{\lambda_{irr}}$ = 0.019 ± 3.71 x 10^{-3} (Fig.5, Table 3). These values were consistently lower than those obtained for the reverse quantum yield ($\Phi_{B\rightarrow A}^{\lambda_{irr}}$). The values of $\Phi_{B\rightarrow A}^{\lambda_{irr}}$ undergo however a 30–fold increase in the irradiation wavelengths range situated between 240 and 480 nm. Overall, the irradiation wavelength correlates linearly with the quantum yield ratios, $\Phi_{B\rightarrow A}^{\lambda_{irr}}/\Phi_{A\rightarrow B}^{\lambda_{irr}}$, that vary between 1.75 and 6.75 (Fig.6).

This relationship (Fig.6) does not support the existence of a common excited–state species that would be generated by the excitation of either Z–SUT or E–SUT as suggested by Kasha's rule

372 which predicts a wavelength–independent quantum yield ratio. A similar behaviour has been
373 observed for photoisomerization of Montelukast in ethanolic solutions [17].

374 The reverse (E → Z) quantum values are well formalised by a sigmoid pattern (Eq.11, Fig.5),

375

376 $$\Phi_{B\to A}^{\lambda_{irr}} = 0.064 + \frac{0.73}{1 + 1300 \times e^{-0.03\times(\lambda_{irr}-300)}} \qquad (11)$$

377

378 Eq.11 allows predicting and estimating the values of the reverse quantum yield at any
379 wavelength in the range situated between 340 and 480 nm (Inset of Fig.5).

380

381 The E → Z phototransformation efficiency (6–7 x 10^{-3} for λ_{irr} < 260 nm) is lower than the
382 average recorded value of the forward photoisomerization (0.019). These results clearly
383 indicate that the lowest–energy excited–states of the E-SUT molecule are much more efficient
384 than its higher–energy ones. This pattern has also been observed for Nifedipine and
385 Montelukast molecules, which are characterised by different structures and photodegradation
386 mechanisms [16,21]. Therefore, the E→ Z (trans → cis) photoisomerizations, as should typically
387 be unimolecular photoreactions, must *a priori* be considered wavelength–dependent.

388

389 The kinetic method used here is found to be very efficient and reliable for relatively quick
390 quantum yield determination. Its advantage is to take into account all absorbing species
391 involved in the photoreactive systems, a parameter that might not always be taken into

consideration by classical methods employed for the determination of photoreaction quantum yields.

3.4. SUT-actinometer

Freshly made Z–SUT solutions were individually investigated under monochromatic irradiation beams of varying radiant power values for a set of ten excitation wavelengths which altogether cover most of SUT absorption spectrum (Table 4). For a given λ_{irr}, the obtained experimental kinetic traces for the series "$j \geq 4$" radiant power values were all fitted with the model Eq.1 (Fig.7). The good fit of the experimental data by the model equation for any wavelength and/or radiant power values confirms the Φ–order nature of SUT kinetics. Linear relationships have been obtained for the variation of the overall rate–constant and radiant power values for each λ_{irr} (Table 4). This behaviour predicted by Eq.2, leads to the determination of the $\beta_{\lambda_{irr}}$ factors as the slopes of the lines. The $\beta_{\lambda_{irr}}$ factors, which have constant values for a given λ_{irr}, are not necessarily linearly correlated to the quantum yields as inferred from Eq.2. However, our experimental results show a good double linear correlation of the $\beta_{\lambda_{irr}}$ factors with the irradiation wavelength, λ_{irr}, Fig.8.

Accordingly, the values of the $\beta_{\lambda_{irr}}$ factor can be determined at any given wavelength within the selected ranges 320–420 nm and 420–480 nm using the appropriate equation relative to either $\beta_{320-420}$ or $\beta_{420-480}$ as given in Fig.8.

From an application point of view, the equations of the latter $\beta_{\lambda_{irr}}$ factors constitute a fundamental element for the development of an actinometric method employing SUT photodegradation reaction. Indeed, the value of the radiant power can be obtained from a rearranged Eq.2 for both spectral sections, as

$$P^{unk.}_{320-420} = \frac{\kappa^{\lambda_{irr}}_{A\rightarrow B}}{52.31\times\lambda_{irr}-15956} \quad \text{and} \quad P^{unk.}_{420-480} = \frac{\kappa^{\lambda_{irr}}_{A\rightarrow B}}{42.23\times\lambda_{irr}+23782} \qquad (12a,b)$$

This means that the actinometric method using SUT photoisomerization reaction in ethanol could readily be implemented for any unknown source of light radiation for the range 320–480 nm. It would be performed by (**1**) subjecting a Z–SUT (*c.a.* 9 x 10^{-6} M) solution in ethanol to a monochromatic beam (320 < λ_{irr} < 480 nm) and collecting its kinetic trace to completion. Then (**2**) the experimental kinetic profile is fitted to Eq.1 and the corresponding overall rate–constant value is extracted. Finally, (**3**) the radiant power value of the unknown source ($P^{unk.}_{\lambda_{irr}}$) is derived from one of Eqs.12.

This straightforward actinometric method should also be applicable to $P^{unk.}_{\lambda_{irr}}$ of a different magnitude to those used in Table 4 [16,17]. In addition, this actinometric method presents the advantage to be implemented without necessarily knowing any of the reactions' attributes such as the reaction quantum yields and/or the spectrum of the photoproduct, and its results for SUT can be combined to other already existing actinometers to widen the dynamic range which can span the 260–570 nm spectral region, using SUT, Montelukast, nifedipine and a diaryethene actinometers [17,21,26]. In principle, the approach can be applied to develop new

434 actinometers obeying similar types of mechanisms to those of the aforementioned drugs (i.e.
435 unimolecular or photoreversible reactions). SUT and the examples we have studied in our team
436 could be viewed as better alternatives to the ICH recommended procedure and quinine
437 hydrochloride actinometry [14,15,21,27-30].

438

4. Conclusion

Φ–order kinetic equations described well the kinetic behaviour of SUT AB(2Φ) photodegradation reaction performed under non-isosbestic irradiation. It confirmed the view that the photodegradation reaction of drugs are better described and rationalised by Φ–order kinetics which should replace the approximate thermal reaction orders' equations and treatments.

The two general methods applied here for the determination of the quantum yields and the assessment of the actinometric potential of the drug are not only easy-to-implement but they also allow generating reliable and quantitative data on the photodegradation reaction. It has become apparent that the $\beta_{\lambda_{irr}}$ factor might be considered as a more relevant parameter than the photochemical quantum yields for the description of drug reactivity as the former is more inclusive, encompassing the latter. In any case, these methods can be employed for the investigation of many other systems and drugs to improve their characterisation and evaluate their properties (such as actinometry).

References

[1] D.B. Mendel, A.D. Laird, X. Xin, S.G. Louie, J.G. Christensen, G. Li., R.E. Shrek, T.J. Abrams, T.J. Ngai, L.B. Lee, L.J. Murray, J. Carver, E. Chan, K.G. Moss, J.O. Haznedar, J. Sukbuntherng, R.A. Blake, L. Sun, C. Tang, T. Miller, S. Shirazian, G. McMahon, J.M. Cherrington, In vivo antitumor activity of SU11248, a novel tyrosine kinase inhibitor targeting vascular endothelial growth factor and platelet-derived growth factor receptors: determination of a pharmacokinetic/pharmacodynamic relationship, Clin. Cancer Res. 9 (2003) 327-337.

[2] G.D. Demetri, A.T. Van Oosterom, C.R. Garrett, M.E. Blackstein, M.H. Shah, J. Verweij, G. McArthur, I.R. Judson, M.C. Heinrich, J.A. Morgan, J. Desai, C.D. Fletcher, S. George, X. Bello, C.M. Baum, P.G. Casali, Efficacy and safety of sanitinib in patients with advanced gastrointestinal stromal tumor after failure of imatinib: a randomised controlled trial, Lancet. 368 (2006) 1329-1338.

[3] A. Haouala, B. Zanolari, B. Rochat, M. Montemurro, K. Zaman, M.A. Duchosal, H.B. Ris, S. Leyvraz, N. Widmer, L.A. Decosterd, Therapeutic Drug Monitoring of the new targeted anticancer agents imatinib,nilotinib, dasatinib, sunitinib, sorafenib and lapatinib by LC tandem mass spectrometry, J. Chromatogr. B. 877 (2009) 1982-1996.

[4] V.R. Adams, M. Leggas, Sunitinib malate for the treatment of metastatic renal cell carcinoma and gastrointestinal stromal tumors, Clin. Ther. 29 (2007) 1338-1353.

[5] E. Raymond, L. Dahan., J.L. Raoul, Y.J. Bang, I. Borbath, C. Lombard-Bohas, J. Valle, P. Metrakos, D. Smith, A. Vinik, J.S. Chen, D. Horsch, P. Hammel, B. Wiedenmann, E. Van Cutsem, S. Patyna, D.R. Lu, C. Blanckmeister, R. Chao, P. Ruszniewski, Sunitinib malate for the treatment of pancreatic neuroendocrine tumors, New Engl. J. Med. 364 (2011) 501-513.

[6] N.A.G. Lankheet, C.U. Blank, H. Mallo, S. Adriaansz, H. Rosing, J.H.M. Schellens, A.D.R. Huitema, J.H. Beijnen, Determination of sunitinib and its active metabolite N-desethylsunitinib in sweat of patients, J. Anal. Toxicol. 35 (2011) 558-565.

[7] EMEA, European public assessment reports, (2006), http://www.ema.europa.eu/docs/en_GB/document_library/EPAR_-_Scientific_Discussion/human/000687/WC500057733.pdf

[8] Y. Zhao, J. Sukbuntherng, L. Antonian, Simultaneous determination of Z-SU5416 and its interconvertible geometric E-isomer in rat plasma by LC/MS/MS, J. Pharm. Biomed. Anal. 25 (2004) 513-522.

[9] F. Navid, R. Christensen, P. Minkin, C.F. Stewart, W.L. Furman, S. Baker, Stability of sunitinib in oral suspension, Oncology. 42 (2008) 962-966.

[10] P. Minkin, M. Zhao, Z. Chen, J. Ouwerkerk, H. Gelderblom, S.D. Baker, Quantification of sunitinib in human plasma by high-performance liquid chromatography-tandem mass spectrometry, J. Chromatogr. B. 874 (2008) 84-88.

[11] Q. Zhou, J.M. Gallo, Quantification of Sunitinib in mouse plasma, brain tumor and normal brain using liquid chromatography-electrspray ionization-tandem mass spectrometry and pharmacokinetic application, J. Pharm. Biomed. Anal. 51 (2010) 958-964.

[12] K. Sidoryk, M. Malinska, K. Bankowski, M. Laszcz, M. Bodziachowska-Panfil, M. Kossykowska, T. Giller, A. Kutner, K. Wozniak, Physicochemical characteristics of sunitinib malate and its process-related impurities, J. pharm. Sci. 102 (2013) 706-716.

[13] L. Ming, Organic Chemistry of drug degradation, RSC Drug Discovery Series No.29, The Royal Society of Chemistry, Cambridge, 2012.

[14] J.T. Piechocki, K. Thoma, Pharmaceutical Photostability and Photostabilisation Technology, Informa Healthcare, London, 2010.

[15] H.H. Tonnesen, Photostability of Drugs and Drug Formulations, second ed., CRC Press, London, 2004.

[16] M. Maafi, W. Maafi, Φ-order kinetics of photoreversible drug reactions, Int. J. Pharm. 471 (2014) 536-543.

[17] M. Maafi, W. Maafi, Montelukast photodegradation: Elucidation of Φ-order kinetics, determination of quantum yields and application to actinometry, Int. J. Pharm. 471 (2014) 544-552.

[18] N. Fomina, J. Sankaranarayanan, A. Almutairi, Photochemical mechasnisms of light-triggered release from nanocarriers, Adv. Drug Delivery Rev. 64 (2012) 1005-1020.

[19] B.M. Wohl, J.F.J. Engebersen, Responsive layer-by-layer materials for drug delivery, J. Control. Release. 158 (2012) 2-14.

[20] I. Tomatsu, K. Peng, A. Kros, Photoresponsive hydrogels for biomedical applications, Adv. Drug Delivery Rev. 63 (2011) 1257-1266.

[21] M. Maafi, W. Maafi, Modelling Nifedipine Photodegradation, Photostability and Actinometric Properties, Int. J. Pharm. 456 (2013) 153-164.

[22] M. Maafi, R.G. Brown,The kinetic model for AB(1Φ) systems. A Closed-form integration of the differential equation with a variable photokinetic factor, J. Photochem. Photobiol. A. 187 (2007) 319-324.

[23] M. Maafi, R.G. Brown, General analytical solutions for the kinetics of AB(k,Φ) and ABC(k,Φ) systems, Int. J. Chem. Kinet. 37 (2005) 162-174.

[24] M. Maafi, R.G. Brown, Analysis of diarylnaphthopyran kinetics. Degeneracy of the kinetic solution, Int. J. Chem. Kinet. 37 (2005) 717-727.

[25] J. Singh, Photochemistry and Pericyclic Reactions, New Age International, New Delhi, 2005.

[26] M. Maafi, The potential of AB(1Φ) systems for direct actinometry. Diarylethenes as successful actinometers for the visible range, Phys. Chem. Chem. Phys. 12 (2010) 13248–13254.

[27] ICH, Guidance for industry Q1B photostability testing of new drug substances and products, Fed. Reg. 62 (1996) 27115-27112.

[28] S.W. Baertschi, Commentary on the quinine actinometry system described in the ICH draft guideline on photostability testing of new drug substances and products, Drug Stab. 1 (1997) 193-195.

[29] S.W. Baertschi, K.M. Alsante, H.H. Tonnesen, A critical assessment of the ICH guideline on photostability testing of new drug substances and products (Q1B): recommendation for revision, J. Pharm. Sci. 99 (2010) 2934-2940.

[30] C.A. De Azevedo Filho, D. De Filgueiras Gomes, J.P. De Melo Guedes, R.M.F. Batista, B.S. Santos, Considerations on the quinine actinometry calibration method used in photostability testing of pharmaceuticals, J. Pharm. Biomed. Anal. 54 (2011) 886-888.

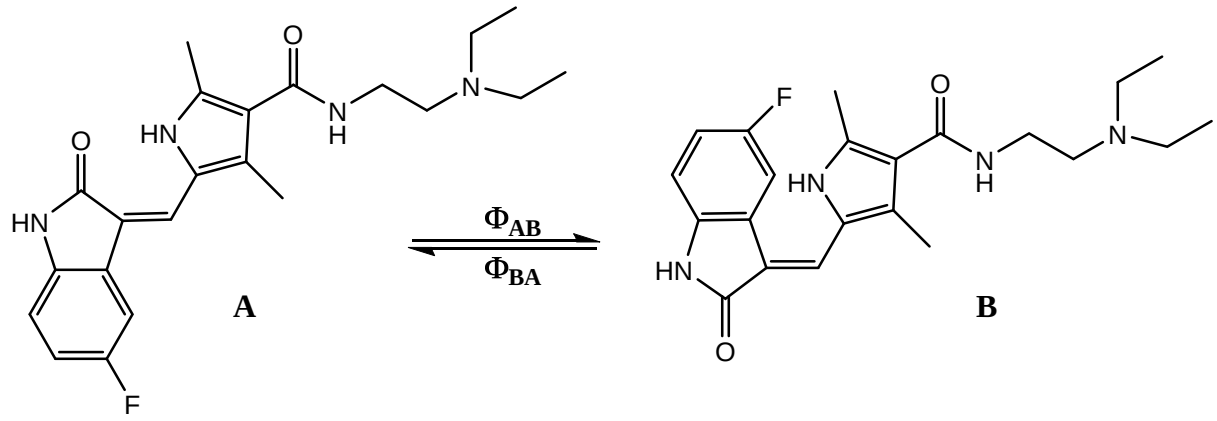

Scheme 1. Reversible photoisomerization of Z-SUT (A) and E-SUT (B).

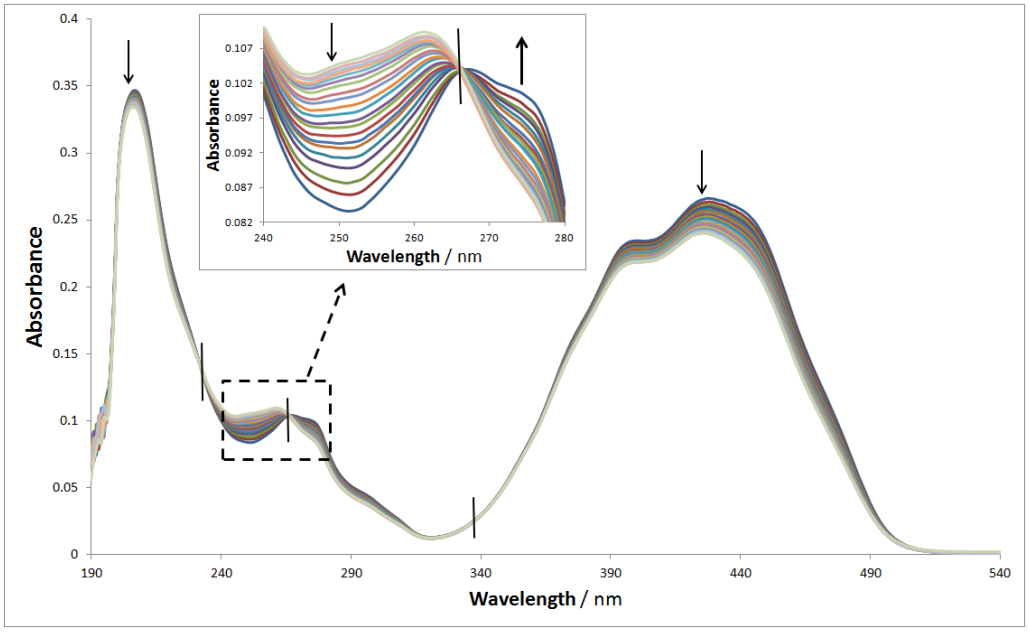

Fig. 1: Evolution of the electronic absorption spectrum of 8.94 x 10^{-6} M Sunitinib (SUT) in ethanol, when irradiated continuously with a monochromatic beam at 430 nm (4.10 x 10^{-6} einstein s^{-1} dm^{-3}, 22°C) for 1200 s. The arrows and vertical lines indicate the direction of the absorbance change and the isosbestic points, respectively.

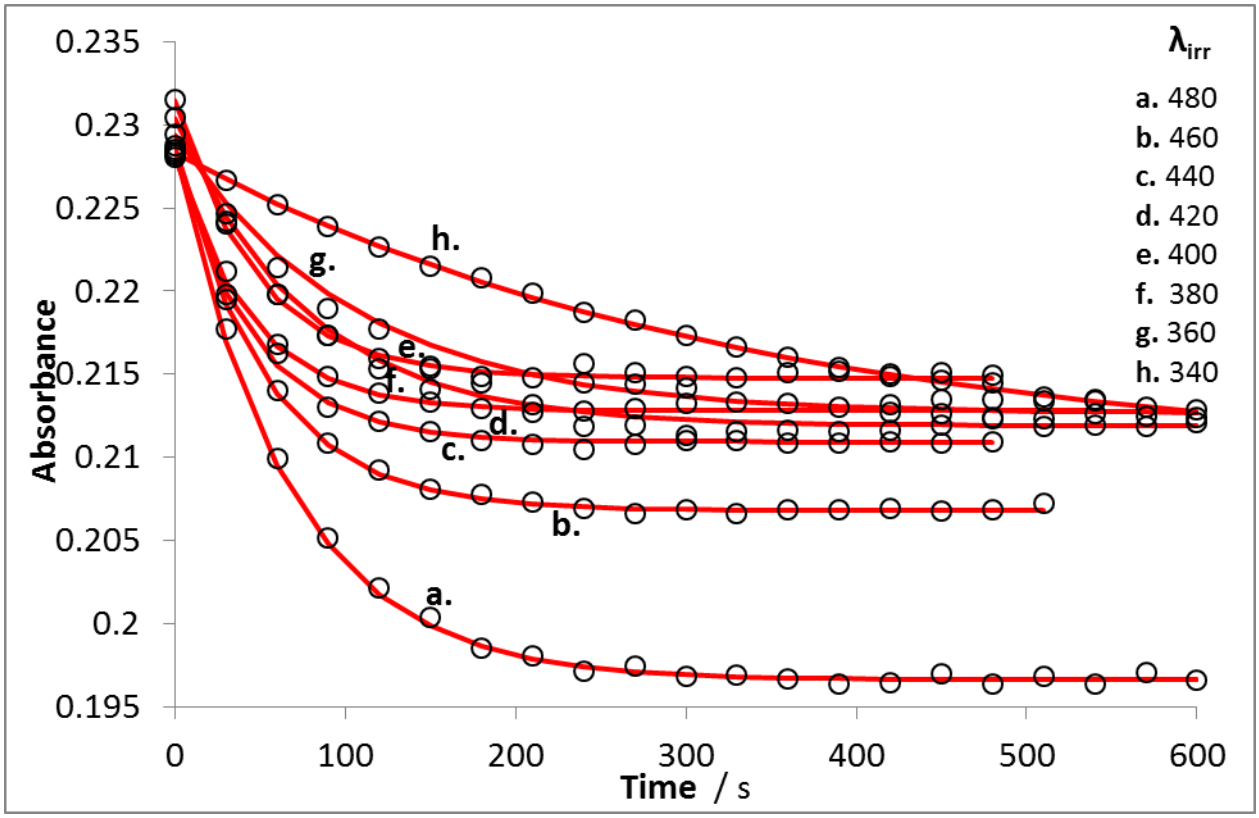

Fig. 2: Photokinetic traces of SUT in ethanol (8.94 x 10^{-6} M) at different irradiation wavelengths (λ_{irr} = 480, 460, 440, 420, 400, 380, 360 and 340 nm) observed at λ_{obs} = 445 nm. Circles represent experimental data and the solid lines are the fitting of the traces with Eq.1.

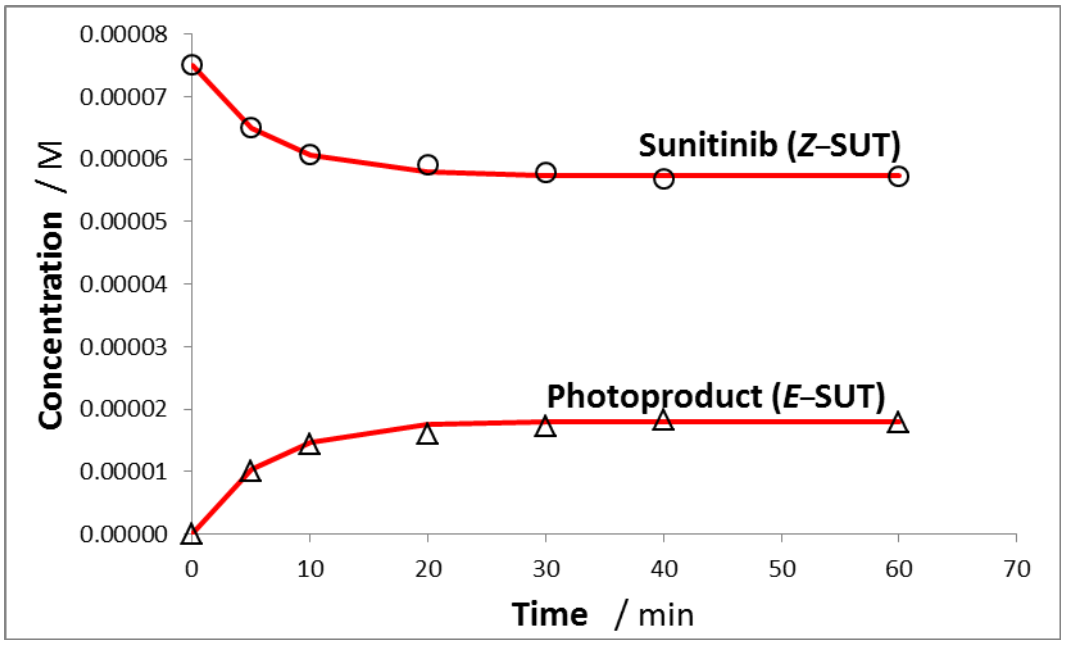

Fig. 3: Evolution of Z–SUT concentration ($C_A(0)$= 7.53 x 10^{-5} M, $C_A(pss)$ = 5.73 x 10^{-5} M) over photodegradation time and formation of the photoproduct (E–isomer, $C_B(pss)$ = 1.8 x 10^{-5} M) monitored by HPLC when irradiated continuously with a monochromatic beam at 345 nm (2.19 x 10^{-6} einstein s^{-1} dm^{-3}, 22°C).

577

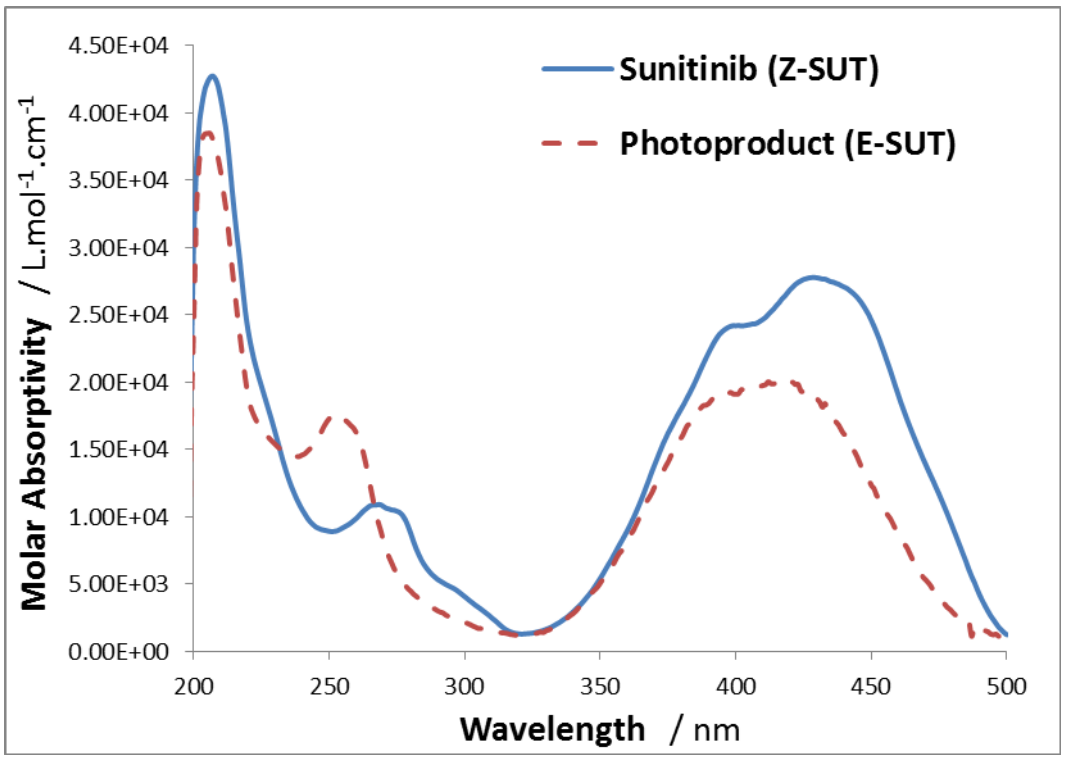

578

579 **Fig. 4**: Native and reconstructed electronic absorption spectra (absorption coefficient units) of
580 Z–SUT and its photoproduct (E–isomer), respectively.

581

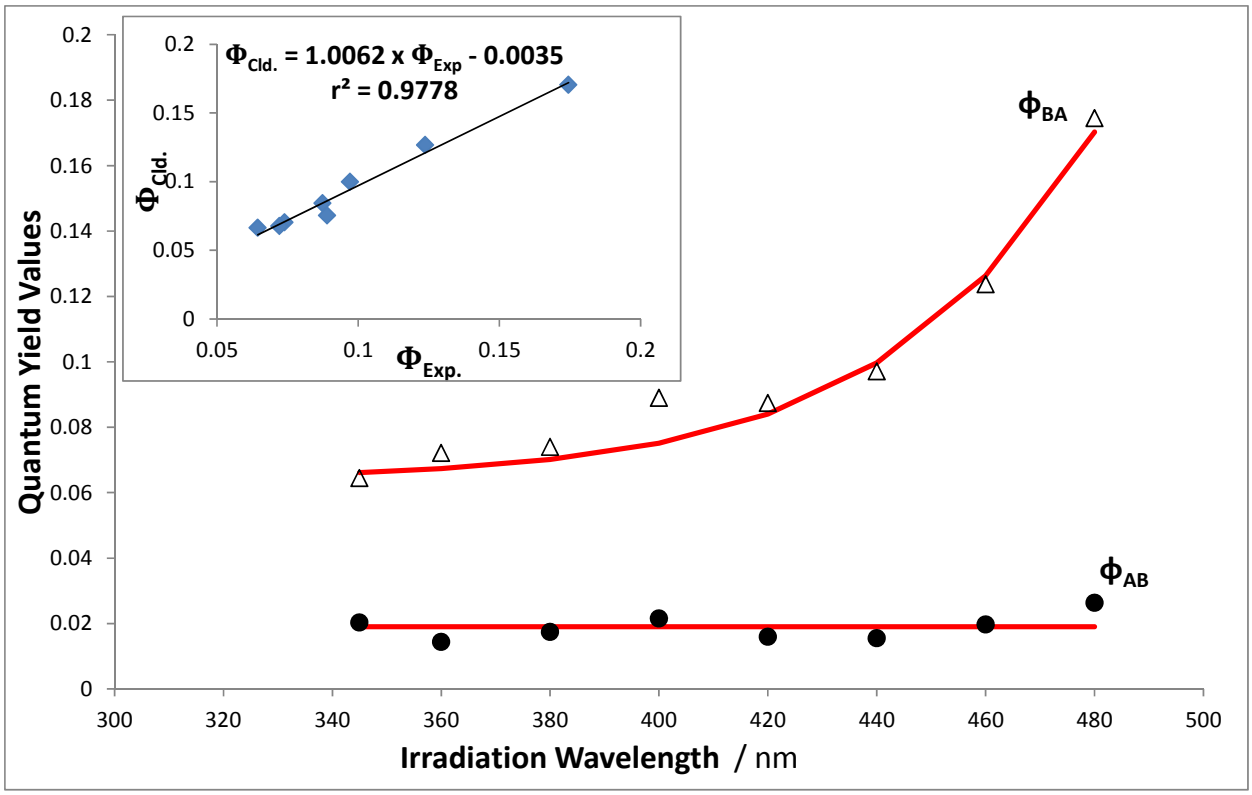

Fig. 5. Average forward ($\Phi_{A\rightarrow B}^{\lambda_{irr}}$) (plain circles) and reverse ($\Phi_{B\rightarrow A}^{\lambda_{irr}}$) (open triangles) quantum yields calculated for irradiation wavelengths (480–340 nm). The lines correspond to the average value of $\Phi_{A\rightarrow B}^{\lambda_{irr}}$, and to the sigmoid relationship, Eq.11, for $\Phi_{B\rightarrow A}^{\lambda_{irr}}$. Inset: the linear–relationship of the experimental and calculated (Eq.11) values (number of data point, n = 8) of the reverse ($\Phi_{B\rightarrow A}^{\lambda_{irr}}$) quantum yield.

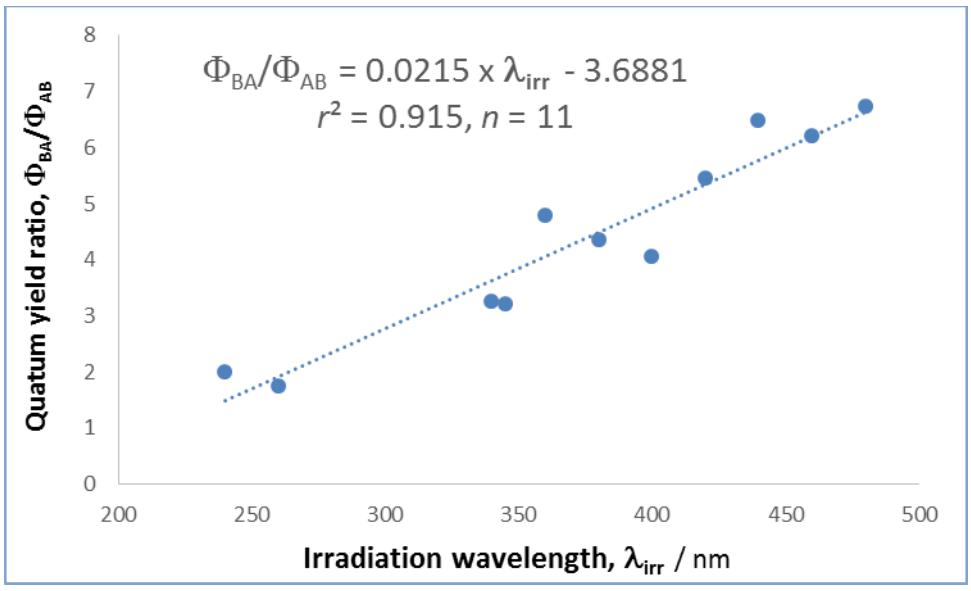

Fig. 6. Linear correlation of the quantum yields ratio ($\Phi_{B\rightarrow A}^{\lambda_{irr}}/\Phi_{A\rightarrow B}^{\lambda_{irr}}$) with irradiation wavelength.

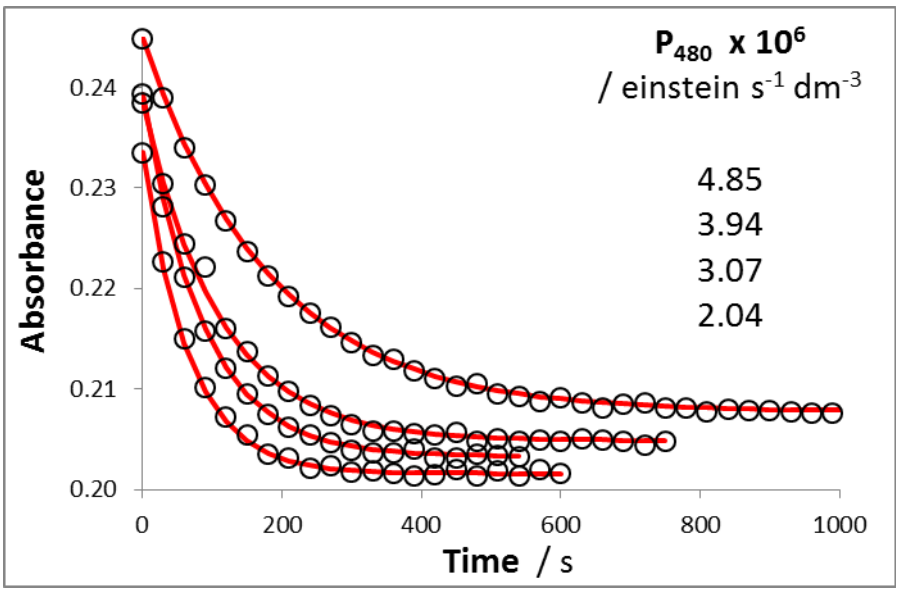

Fig.7. Effect of increasing radiant power values ($P_{\lambda_{irr}}$) of the monochromatic irradiation beam on the kinetic traces of SUT (8.94 x 10^{-6} M), $\lambda_{irr} = \lambda_{obs}$ = 480 nm. Circles represent experimental data and the solid lines correspond to the fitting of the traces with the AB(2Φ) kinetic model, Eq.1.

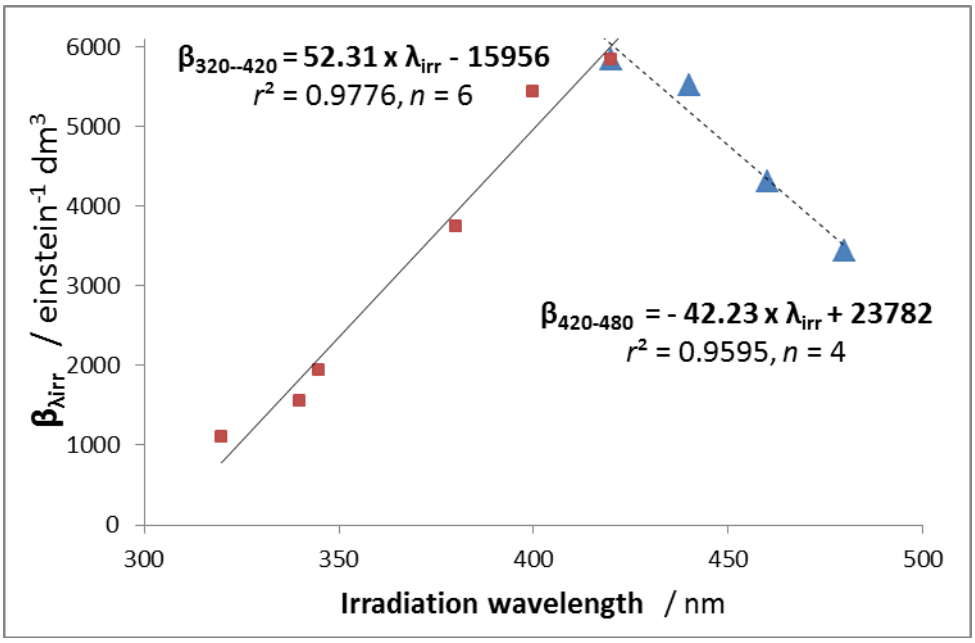

Fig. 8: Correlation of $\beta_{\lambda_{irr}}$ (Table 4) with irradiation wavelength (λ_{irr}).

Table 1

Overall photoreaction rate–constants, spectroscopic and kinetic parameter values of SUT for a set of monochromatic irradiations performed in ethanol at 22°C**.**

λ_{irr} /nm	$A_{tot}^{\lambda_{irr}/445}(0)$	$P_{\lambda_{irr}}$ x 10^6 /Einstein.s^{-1}.dm^{-3}	$A_{tot}^{\lambda_{irr}/\lambda_{irr}}(pss)$	$k_{A\rightarrow B}^{\lambda_{irr}}$ / s^{-1}
480	0.229	4.85	0.058	0.0155
460	0.229	4.30	0.145	0.0195
440	0.228	4.07	0.221	0.0225
420	0.233	3.93	0.237	0.023
400	0.239	3.48	0.219	0.021
380	0.243	2.97	0.167	0.013
360	0.247	2.67	0.085	0.0094
340	0.240	1.98	0.028	0.003
260	0.214	1.16	0.086	0.00064
240	0.215	1.22	0.093	0.00057

Table 2

Quantum yields, equilibrium constant $K_{A\rightarrow B}^{\lambda_{isos}}$ and overall rate–constant values for the photodegradation of SUT under isosbestic monochromatic irradiation conditions. [a)] (the labels *A* and *B* represent Z–SUT and E–SUT, respectively).

λ_{isos} /nm	C_A (0) / M	$l_{\lambda_{isos}}$ / cm	$l_{\lambda_{obs}}$ / cm	$C_A(pss)$ / M	$C_B(pss)$ / M	$P_{\lambda_{isos}}$ /einstein.s^{-1}.dm^{-3}	$F_{\lambda_{isos}}$	$k_{A\rightarrow B}^{\lambda_{isos}}$ / s^{-1}	$\Phi_{A\rightarrow B}^{\lambda_{isos}}$	$\Phi_{B\rightarrow A}^{\lambda_{isos}}$	$K_{\rightleftharpoons}^{\lambda_{isos}}$
345	7.53x10^{-5}	2	1	5.73 x10^{-5}	1.8x10^{-5}	2.19x10^{-6}	1.63	2.83x10^{-3}	0.02	0.064	0.315

a) $l_{\lambda_{isos}}$ = 2 cm and $l_{\lambda_{obs}}$ = 1cm.

Table 3

Quantum yields, overall rate–constant, absorption coefficients and initial velocity values for SUT photodegradation reactions under various monochromatic irradiations. (*A* and *B* correspond respectively to Z–SUT and E–SUT).

λ_{irr} /nm	$P_{\lambda_{irr}}$ x 10^6 /einstein. $s^{-1}.dm^{-3}$	$A_{SUT}^{\lambda_{irr}/443}(pas)$ [a]	$k_{A\rightarrow B}^{\lambda_{irr}}$ / s^{-1}	$r_0^{\lambda_{irr}/443}$ / s^{-1}	$\varepsilon_A^{\lambda_{irr}}$ / $M^{-1}.cm^{-1}$	$\varepsilon_B^{\lambda_{irr}}$ / $M^{-1}.cm^{-1}$	$F_{\lambda_{irr}}(0)$	$\Phi_{A\rightarrow B}^{\lambda_{irr}}$ [a,b]	$\Phi_{B\rightarrow A}^{\lambda_{irr}}$
480	4.85	0.198	0.0155	-4.74×10^{-4}	9234	2911	1.93	0.026 ± 7.39×10^{-4}	0.175 ± 1.26×10^{-2}
460	4.30	0.208	0.0195	-4.09×10^{-4}	19048	8657	1.60	0.020 ± 3.63×10^{-3}	0.124 ± 1.26×10^{-2}
440	4.07	0.211	0.0225	-3.76×10^{-4}	27078	16133	1.39	0.015 ± 2.44×10^{-3}	0.097 ± 2.56×10^{-3}
420	3.93	0.233	0.023	-3.52×10^{-4}	26882	19993	1.37	0.016 ± 2.68×10^{-3}	0.087 ± 2.60×10^{-3}
400	3.48	0.239	0.021	-3.56×10^{-4}	24202	19116	1.43	0.022 ± 7.87×10^{-3}	0.089 ± 2.79×10^{-3}
380	2.97	0.243	0.013	-2.51×10^{-4}	18084	15922	1.59	0.017 ± 2.77×10^{-3}	0.074 ± 4.94×10^{-3}
360	2.67	0.226	0.0094	-1.92×10^{-4}	8993	8276	1.90	0.014 ± 4.06×10^{-3}	0.067 ± 1.78×10^{-2}
345	2.04	0.209	0.0035	-7.49×10^{-5}	4021	3863	2.12	0.020 ± 6.47×10^{-4}	0.064 ± 2.05×10^{-3}
340	1.98	0.221	0.003	-5.89×10^{-5}	2950	2817	2.17	0.020 ± 8.79×10^{-4}	0.065 ± 2.79×10^{-3}
260	1.16	0.214	0.00064	-1.74×10^{-5}	9894	16266	1.93	0.004 ± 1.24×10^{-4}	0.007 ± 2.57×10^{-4}
240	1.22	0.215	0.00057	-1.06×10^{-5}	10529	14604	1.92	0.003 ± 2.62×10^{-4}	0.006 ± 7.17×10^{-4}

[a] $l_{\lambda_{443}}$ = 2 cm. [b] $l_{\lambda_{irr}}$ = 1cm.

633

634

635 **Table 4**

636 Correlation equations for the variation of SUT photodegradation overall rate–constants ($k_{A\rightarrow B}^{\lambda_{irr}}$) with
637 radiant power ($P_{\lambda_{irr}}$), the corresponding $\beta_{\lambda_{irr}}$ factor values, and the span of radiant power employed for
638 various monochromatic irradiations.

Irradiation wavelength λ_{irr} / nm	**Equation of the line**[a,b] $k_{A\rightarrow B}^{\lambda_{irr}} = \beta_{\lambda_{irr}} \times P_{\lambda_{irr}} + \mathbf{intercept}$	**Correlation coefficient,** r^2	$P_{\lambda_{irr}}$ **x** 10^6 / einstein.s^{-1} .dm^{-3}
480	3437.7 x P_{480} – 0.0013	0.9980	2.04 – 4.85
460	4301.4 x P_{460} + 0.001	0.9887	1.80 – 4.30
440	5521.9 x P_{440} + 0.0006	0.9882	1.77 – 4.07
420	5846.6 x P_{420} + 0.006	0.9851	1.66 – 3.93
400	5432.6 x P_{400} + 0.0023	0.9718	1.45 – 3.48
380	3740.9 x P_{380} + 0.0019	0.9959	1.19 – 2.97
360	5866.2 x P_{360} – 0.0064	0.9915	1.58 – 2.67
345	1938.1 x P_{345} – 0.0004	0.9941	1.42 – 2.04
340	1560.1 x P_{340} – 0.00007	0.9881	0.85 – 1.98
320	1096.2 x P_{320} + 0.00001	0.9954	0.61– 1.33

639 [a] $k_{A\rightarrow B}^{\lambda_{irr}}$ and intercepts expressed in s^{-1} and $\beta_{\lambda_{irr}}$ in $einst^{-1}.dm^3$. [b] The number of data
640 points (*n*) used for the graphs were in the range $7 \geq n \geq 4$.

641